

An ISO/SWS study of the dust composition around S stars^{*}

A novel view of S-star dust

S. Hony¹, A. M. Heras², F. J. Molster³, K. Smolders⁴

¹ Laboratoire AIM, CEA/DSM - CNRS - Université Paris Diderot, DAPNIA/Service d'Astrophysique, Bât. 709, CEA-Saclay, F-91191 Gif-sur-Yvette Cédex, France

² Research and Scientific Support Department-ESA/ESTEC, P.O. Box 299, 2200 AG Noordwijk, The Netherlands

³ NOVA, P.O. Box 9513, 2300 RA Leiden, The Netherlands

⁴ Instituut voor Sterrenkunde, K.U. Leuven, Celestijnenlaan 200D, B-3001 Leuven, Belgium

received October 26, 2021; accepted date

Abstract

Aims. We investigate the composition of the solid-state materials in the winds around S-type AGB stars. The S stars produce dust in their wind that bears a resemblance to the dust produced in some O-rich AGB stars. However, the reported resemblance is mostly based on IRAS/LRS spectra with limited spectral resolution, sensitivity, and wavelength coverage.

Methods. We investigate the dust composition around S stars using ISO/SWS data that surpass the previous studies in terms of spectral resolution and wavelength coverage. We selected the dust producing S stars in the ISO/SWS archive with enough signal to perform a detailed dust analysis, and then compare the dust spectra from the 9 sources with the O-rich AGB spectra and a subset of M super-giants. We constructed average dust emission spectra of the different categories.

Results. We report the discovery of several previously unreported dust emission features in the S star spectra. The long wavelength spectra of W Aql and π^1 Gru exhibit the “30” μm feature attributed to MgS. Two sources exhibit a series of emission bands between 20 and 40 μm that we tentatively ascribe to Diopside. We show that the 10–20 μm spectra of the S stars are significantly different from the O-rich AGB stars. The O-rich stars exhibit a structured emission feature that is believed to arise from amorphous silicate and aluminium-oxide. The S stars lack the substructure found in the O-rich stars. Instead they show a smooth peak with a varying peak-position from source to source. We suggest that this feature is caused by a family of related material, whose exact composition determines the peak position. The observed trend mimics the laboratory trend of non-stoichiometric silicates. In this scenario the degree of non-stoichiometry is related to the Mg to SiO₄ ratio, in other words, to the amount of free O available during the dust grain growth.

Key words. Stars: mass-loss – Stars: AGB and post-AGB – circumstellar matter – supergiants – Infrared: stars

1. Introduction

Asymptotic giant branch (AGB) stars are evolved stars of low to intermediate mass in the ZAMS mass range of ~ 1 to $8 M_{\odot}$. During the AGB phase, these stars are typified by high luminosity and low surface temperature, which implies a very large radius and low surface gravity. These stars often exhibit substantial mass loss through a dust driven or pulsation driven wind. This mass loss is important for several reasons. *i)* These winds provide the means through which these stars return nucleosynthesis products (i.e. metals) from the interior of the star into the interstellar medium (ISM). As the bulk of all stars fall in this mass range, the winds of AGB stars are one of the dominant contributors to the enrichment of the ISM. *ii)* These dusty winds alter the appearance of these stars because they cause the star to be surrounded by an envelope of gas and dust. The dust will absorb the stellar radiation and reradiate in the IR; therefore if one is to study the properties of these stars, the dusty envelope needs to be taken into account. *iii)* The further evolution of the star is de-

termined by the mass loss. Unlike most types of stars, AGB star evolution is not determined by the nuclear fusion processes in the interior but by the mass loss at the surface and the AGB will end when the reservoir of envelope material has been exhausted by the mass loss.

The type of molecules and solid-state particles that are present in the winds are to the first order determined by the elemental abundances at the surface of the star. Most important in this respect is the number ratio of C-atoms to O-atoms (C/O ratio), because the carbon-monoxide (CO) molecule is easily formed and very stable. This causes most of the C- and O-atoms to be present in the form of CO. These atoms are then effectively not taking part in the chemistry and dust- condensation that occurs in these surroundings. Only the fraction of either O-atoms if C/O is smaller than unity, or C-atoms if C/O exceeds unity, is available. This dichotomy as a function of C/O ratio is clearly found in the AGB stars. When $C/O < 1$, i.e. in O-rich AGB stars, one finds large amounts of oxygen-bearing molecules, like SiO, H₂O and CO₂, while for $C/O > 1$, i.e. in C-rich AGB stars, molecules like CH, C₂H₂ and HCN are present. The same holds for the composition of the dust around these objects. The O-rich stars exhibit silicates and oxides like amorphous aluminium-oxide (Al₂O₃) or spinel, while their C-rich counterparts produce amorphous carbon, silicon carbide and sulfides like MgS.

Send offprint requests to: S. Hony (sacha.hony@cea.fr)

^{*} based on observations obtained with ISO, an ESA project with instruments funded by ESA Member states (especially the PI countries: France, Germany, the Netherlands and the United Kingdom) and with the participation of ISAS and NASA.

Table 1. Details of the sources/SWS spectra used in this study.

Source	IRAS name	AOT ^a	TDT ^b	Class. ^c	SP98 ^d	Spec.Type ^e	Remarks
S stars from Stephenson (1994) used in this study							
R And	00213+3817	01(2)	40201723	2.SEc	SE3	S3,5-8,8e	18 μ m feat. weak
S Cas	01159+7220	01(2)	41602133	3.SEp	SE3	S3,4-5,8e	15 μ m feat., 18 μ m feat. absent, C ₂ H ₂ +HCN abs.
W Aql	19126-0708	01(2)	16402335	3.SEp	SE3	S3,9-6,9e	15 μ m feat., 18 μ m feat. absent, C ₂ H ₂ +HCN abs.
R Cyg	19354+5005	01(1)	42201625	2.SEb	SE3	S2,5,9-6,9e	18 μ m feat. absent, 10 μ m feat. narrow
χ Cyg	19486+3247	01(2)	15900437	2.SEb	SE3	S6,2-10,4e	18 μ m feat. absent, substructure at 10.2 μ m
AA Cyg	20026+3640	01(2)	36401817	2.M	N	S7,5-7,5,6	:
RZ Sgr	20120-4433	01(2)	14100818	2.SEa	SE2	S4,4ep	:
π^1 Gru	22196-4612	01(2)	34402039	2.SEa	SE2	S7,5e	18 μ m feat. absent
RX Lac	22476+4047	01(1)	78200427	2.SEa	SE1	M7.5Se	:
Stars from Stephenson (1994) not included in the S star sample							
W Cet	23595-1457	01(2)	37802225	2.SEa:	-	S7 ^{e1}	Low SNR
T Cet	00192-2020	01(2)	55502308	2.SEa	SE1t	M5-6S IIe	M supergiant, M, MS or S
RW And	00445+3224	01(3)	42301901	7	SE3:	M5-10e(S6,2e)	Low SNR
WX Cam	03452+5301	01(2)	81002721	1.NO	-	S5/5.5 ^{e2}	Low SNR
NO Aur	05374+3153	01(1)	86603434	2.SEa	SE1	M2S Iab	Supergiant
LY Mus	13372-7136	01(2)	13201304	1.NO	-	M4III ^{e1}	No dust features
II Lup	15954-5114	06	29700401	3.CE ^{c1}	-	SC ^{e3}	Carbon-rich
ST Her	15492+4837	01(3)	41901305	2.SEa	SE1	M6-7 IIIaS	MS
OP Her ^f	17553+4521	01(1)	77800625	1.NO	N	M5 I Ib-IIIa(S)	No dust features
HD 165774	18058-3658	01(2)	14100603	1.NO:	-	M2II/III ^{e1}	No dust features, low SNR
S Lyr	19111+2555	01(1)	52000546	2.CE:	SE2	SCe	Low SNR
HR Peg	22521+1640	01(2)	37401910	1.NO	-	S5,1 ^{e1}	No dust features
GZ Peg	23070+0824	01(3)	37600306	1.NO	N:	M4S III	No dust features
Supergiants with 10 μ m features resembling the S stars							
KK Per	02068+5619	01(1)	45701204	2.SEa	-	M2 Iab	18 μ m feat. weak, UIR
V605 Cas	02167+5926	01(2)	61301202	2.SEa:	-	M2 Iab ^{e4}	18 μ m feat. weak, UIR
AD Per	02169+5645	01(2)	78800921	2.SEap	-	M2.5 Iab ^{e5}	18 μ m feat. weak, UIR
NO Aur	05374+3153	01(1)	86603434	2.SEa	SE1	M2S Iab	18 μ m feat. weak, UIR
V1749 Cyg	20193+3527	01(2)	73000622	2.SEb	SE3t	M3 Iab	UIR
IRC+40 427	20296+4028	01(3)	53000406	2.SEap:	-	M0-2 I ^{e6}	18 μ m feat. absent, UIR
CIT 11	20377+3901	01(1)	40503119	2.SEb	-	M3: Iab	18 μ m feat. weak
V354 Cep	22317+5838	01(2)	41300101	2.SEc	SE6	M2.7 Iab	15 μ m feat., 18 μ m feat. absent
V582 Cas	23278+6000	01(1)	38501620	2.SEc	SE5	M4 I ^{e7}	18 μ m feat. weak, UIR:
Other sources used in this study							
IRC+50 096	03229+4721	01(2)	81002351	3.CE	-	C ^{e2}	Carbon-rich, "30" μ m feature
R Hya	13269-2301	01(1)	08200502	2.SEa	SE2t	M6-9eS(Tc)	
TY Dra	17361+5746	01(2)	74102309	2.SEc	SE8t	M5-8	

^aObserving mode used (see de Graauw et al. 1996; Clegg et al. 1996). Numbers in brackets correspond to the scanning speed. ^bTDT number which uniquely identifies each ISO observation. ^cClassification of the SWS spectrum from Kraemer et al. (2002), except ^{e1}Sloan et al. (2003). ^dIR classification in the scheme of Sloan & Price (1998). ^eSpectral types are from Sloan & Price (1998), except ^{e1}Kharchenko (2001), ^{e2}Buscombe (2001), ^{e3}Buscombe (1998), ^{e4}Humphreys (1970), ^{e5}Blanco (1955), ^{e6}Solf (1978) and ^{e7}Winfrey et al. (1994). ^fThis source is only listed in the first edition of general catalogue of S stars (Stephenson 1995) and is classed M star in the second edition.

During the AGB phase the elemental abundances on the surface of the star are being altered by a process called dredge-up. This causes fusion products from the interior to be transported to the surface, gradually increasing the C/O ratio. So, in the broadest possible terms stars on the AGB gradually evolve from O-rich AGB stars to C-rich AGB stars. In this scenario the S stars form an interesting intermediate class of objects that have $C/O \approx 1$. Simplemindedly, one would assume that in such surroundings the range of molecules and dust components could be very wide perhaps overlapping with both the typical O-rich and C-rich species or species that are not found in either surroundings. Theoretically, iron-silicide and metallic iron are the dust species predicted on the basis on chemical equilibrium calculations (Ferrarotti & Gail 2002). Observationally, this class of objects has not been exhaustively studied to determine the dust composition although some studies have focused on the 10 μ m emission feature from S stars (Little-Marenin & Little 1988; Chen & Kwok 1993; Sloan & Price 1998; Speck et al. 2000).

In particular the spectra obtained with the Short Wavelength Spectrometer (SWS) (de Graauw et al. 1996) on-board the Infrared Space Observatory (ISO) (Kessler et al. 1996) which cover a much broader wavelength range (2–45 μ m) than available before with a high sensitivity and spectral resolving power, allow us to get a more complete picture of the composition around S stars.

The most diagnostic feature in the S star spectra is found in the 10 μ m region. The dust emission features in the 10 μ m region are very extensively studied because *i*) this window is available for ground-based observations, *ii*) it holds the important diagnostic resonances of both O-rich (silicates, Al₂O₃ and spinel) and C-rich (SiC) dust and *iii*) spectra for many evolved stars in this region are available in the form of IRAS/LRS spectra. Many studies have focused on classifying the spectral appearance of the ~ 10 μ m emission band, using various classification schemes, and relating the classification to the other observable characteristic of the sources like the spectral

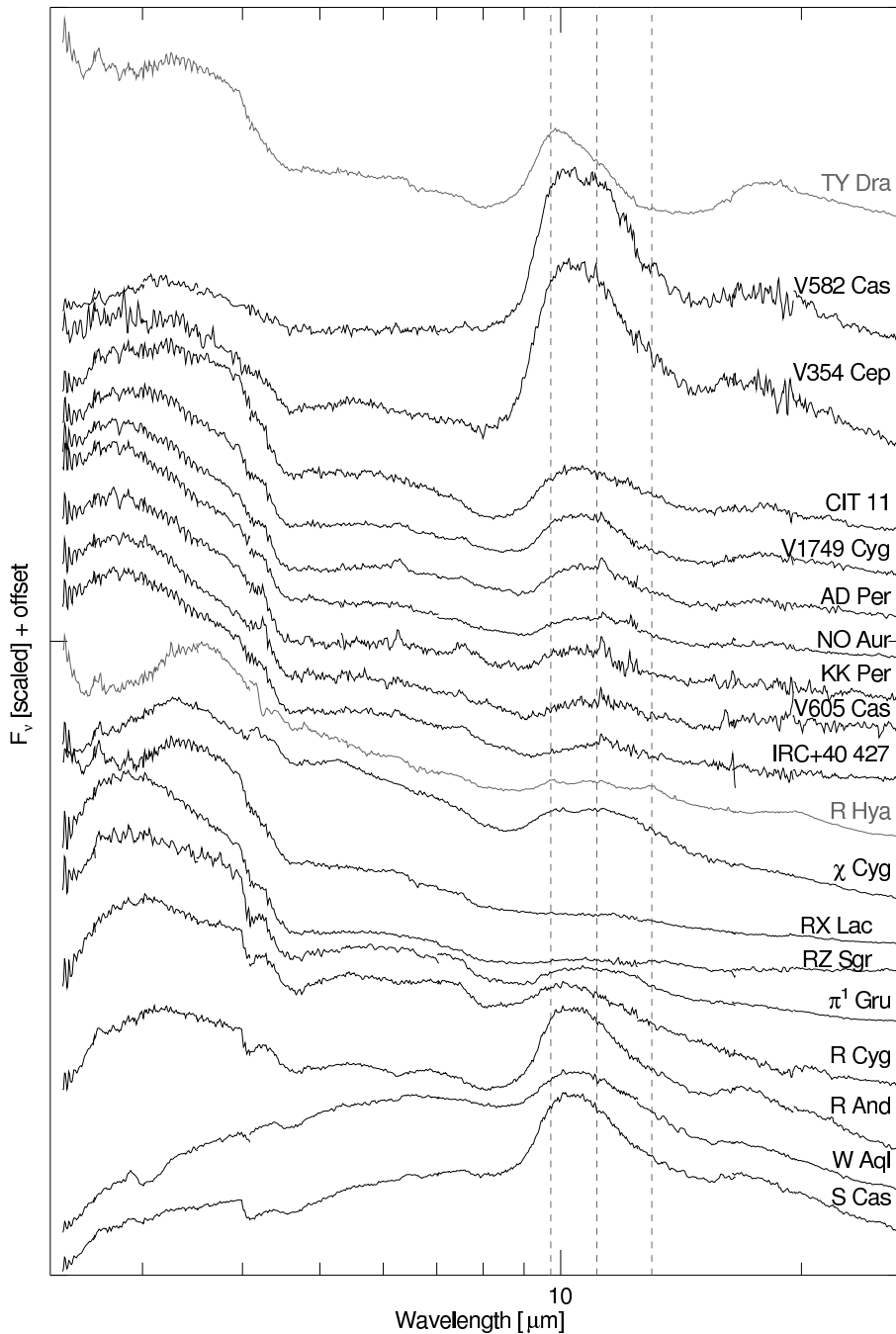


Figure 1. ISO/SWS spectra of the sources listed in Table 1. From the bottom to the top we show. Eight spectra of S stars (S Cas – χ Cyg). The grey spectrum in the middle is R Hya, an O-rich AGB star that shows the typical structured $10 \mu\text{m}$ feature. Then nine M super-giants that exhibit a smooth and displaced $10 \mu\text{m}$ features (IRC+40 427 – V582 Cas). At the very top we show TY Dra as an example of classical silicate dominated spectrum. The dashed lines represent the wavelengths of the substructures found in the O-rich AGB stars.

type, luminosity class, the C/O ratio, the variability type or the mass-loss rate (Little-Marenin & Little 1988; Skinner et al. 1990; Little-Marenin & Little 1990; Chen & Kwok 1993; Sloan & Price 1995, 1998; Sylvester 1999; Speck et al. 2000; Miyata et al. 2000; Kraemer et al. 2002; Yang et al. 2007). Here we do not repeat the details of these studies but focus on the main conclusions that are relevant for the current work and refer to Sloan & Price (1998) and Speck et al. (2000) for extensive and thorough comparisons of the relevant literature and the various interpretations of the dust emission characteristics.

The main points that have emerged are as follows:

1. O-rich AGB stars show a range of dust emission features with a range of peak positions.
 - (a) A single narrow peak at $9.7 \mu\text{m}$ (on a F_ν scale), due to “classical silicates”. The corresponding Si-O bending mode resonance is also observed near $18 \mu\text{m}$.

- (b) A broader structured feature, with local maxima at 9.7 , 11 and $13 \mu\text{m}$, with the peak-position close to $\sim 10 \mu\text{m}$.
- (c) A broad and shifted feature peaking at longer wavelength (up to $13 \mu\text{m}$). This broad feature exhibits the same local maxima as mentioned above. It is generally accepted that this broad feature is due to the dominant contribution of dust components other than the silicates, probably amorphous aluminium-oxide (Onaka et al. 1989).

The origin of the structured features (b) in between the two extremes above is uncertain. While Onaka et al. (1989) and Lorenz-Martins & Pompeia (2000) model these spectra with a mixture of silicates and aluminium-oxide, Egan & Sloan (2001) find that these observations, with the additional constraints set by the IRAS broadband photometry, are best explained using pure silicates in a dust shell of larger optical depth. However, the fact that one finds the same substructure

tures within a wide range of peak-positions argues against the opacity effect being dominant, and most likely these sources represent a mixture of silicate and aluminium-oxide grains.

2. M super-giants exhibit a similar range of 10 μm features, although they are more weighted to the classical silicate profiles (a) and the broad (c)-type features are rare (Sloan & Price 1998). An interesting exception is a significant fraction of M super-giants of the h and χ Per association that exhibit a (c)-type feature peaking near 10.5 μm with the 11.3 μm UIR band perched on top (Sylvester et al. 1998). In Sect. 5 we will compare these interesting sources with the S stars.
3. Little-Marenin & Little (1988) find that S-type stars preferentially exhibit a broad feature peaking in the 10.5–10.8 μm range, which in fact makes them dub this feature the “S” feature. This agrees well with the findings of Sloan & Price (1998), who also find that the S-type stars in their sample predominantly exhibit such a broad feature. In contrast Chen & Kwok (1993) report that the S-type stars have emission features very similar to M stars, covering the complete range from pure silicates to the broad feature profile. This difference is easily understood from the fact that the latter authors include in their much larger sample also many MS and weak S stars which have a C/O ratio well below unity and should have dust similar to the M stars. The profile found in the strong S stars is broad and peaking in the 10.5–10.8 μm range. The extend and peak-position of this S star feature are very similar to the broad features found in the O-rich AGB stars, however the 13 μm feature is lacking in the S star spectra (Sloan & Price 1998, Fig.9). These authors also find that there might be a slight enhancement between 10 to 11 μm in the S-type feature when compared to the M star sample, although they state that the difference might not be significant given the quality of the LRS spectra they used.

In this paper we explore the dust composition around S stars as derived from the available SWS spectra.

2. Observations

The ISO/SWS database contains 22 S star spectra that cover the full wavelength range of 2.3–45 μm : 21 ISO/SWS sources listed in the second edition of the general catalogue of S stars (Stephenson 1994) with the addition of the S star OP Her are given in Table 1. Of these 22 sources we include nine in the S star sample that we explore here; NO Aur is a super-giant, II Lup is carbon-rich, ST Her is an MS star and T Cet is of uncertain nature. The other stars have either no significant dust emission or too little signal-to-noise to investigate their dust composition to the level of detail required here.

2.1. Data reduction

The data were processed using SWS interactive analysis, IA (see de Graauw et al. 1996), using calibration files and procedures equivalent to pipeline version 10.1. Further data processing consisted of extensive bad data removal and rebinning on a fixed resolution ($\lambda/\Delta\lambda=200$) wavelength grid. In order to combine the different sub-bands into one continuous spectrum from 2 to 45 μm we applied scaling factors. In general the match between the different sub-bands is good and the applied scaling/offsets are small compared to the flux calibration uncertainties with a few exceptions:

2.1.1. χ Cyg

The band 2A (4.1–5.3 μm) and 2C (7.0–12.5 μm) data are affected by strong memory effects. The shapes of band 2A of the up and down scans differ substantially. The slope of the band 2C data differs while the details of the shape and substructure are present in both scans. The data appear to be also slightly affected by miss-pointing as we have to apply a scaling of ~ 1.08 to the band 1 (2.4–4.1 μm) data and 1.2 to the band 3 (12.5–29 μm) data.

2.1.2. π^1 Gru

The data for π^1 Gru are apparently affected by a slight miss-pointing and the data for the sub-bands 2A to 3D (4.1 – 27.5 μm) need to be multiplied by a relatively large factor (~ 1.25) to be consistent with the flux levels at shorter and longer wavelengths. We note that the main signature of the MgS feature is contained within sub-band 3D (19.5 – 27 μm) and is not affected by the scaling (see also Fig. 2).

The final reduced spectra are presented in Fig. 1. As it turns out these stars are very rich in their dust emission spectra exhibiting a wide range of dust features from different types of materials. We will first discuss the long wavelength part of the spectra of π^1 Gru, W Aql and RX Lac as they show features that have not been detected before around S stars.

3. Long wavelength spectra

3.1. The “30 μm ” feature

In Fig. 4 we show the spectra of π^1 Gru and W Aql. We also show for comparison the SWS spectrum of the C-rich red giant IRC+50 096, which exhibits purely C-rich dust features and the MS star ST Her, which exhibits O-rich dust features.

The most remarkable feature in the spectra of these two S stars is the emission feature starting at 23.5 μm and peaking at 26 μm , indicated in Fig. 4 with MgS. The feature is weak and even in the closeup of the region in the right panel of Fig. 5 not very prominent. This is probably also the reason why it has eluded detection until now.

In Fig. 2 we display the spectra in intensity units that better reveal the structure in this region. The shape of the feature found in the S star spectra closely corresponds to the shape of the much stronger MgS resonance found in the C-rich star IRC+50 096. In particular the change of slope from 22 to 24 μm and the second change beyond 26 μm is detected in the three sources at the top. We also show the expected spectrum from MgS, which exhibits the same shape. The two independent scans in the SWS data yield the same shape, attesting to the reality of the MgS detection.

The presence of MgS around these stars is unexpected and prompts several questions on dust condensation conditions around such stars. It is important to also take into account other aspects of these systems. First we will discuss the other dust features in the spectra of these stars and subsequently the molecular composition.

3.2. RX Lac and AA Cyg

In Fig. 3 we show the spectra of RX Lac and AA Cyg. Both sources exhibit structure at 20, 32.5 and 40 μm . The structure around 20 μm seems to be quite secure in both spectra. The long wavelength part of the AA Cyg spectrum is very noisy.

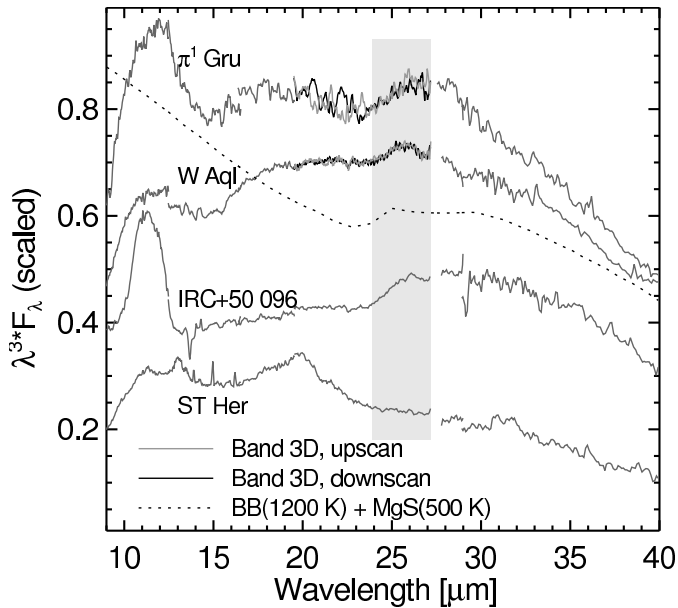


Figure 2. Comparison of the features found in the SWS spectra of π^1 Gru and W Aql to the MgS feature in IRC+50 096. We show the signal of the two independent scans of sub-band 3D. The characteristic sharp rise from 24 to 26 (indicated in the light shaded area) with a gradual decline towards longer wavelength is found in all available scans. The scale along the ordinate is chosen to better bring out the structure in this wavelength domain without having to resort to removing an underlying baseline. The dotted line shows the spectral signature expected from a star surrounded by MgS, simulated with a Planck-function of 1200 K plus the emission of MgS grains at 500 K in a CDE-shape distribution. Near the bottom we show the spectrum of the MS star ST Her as an example of a source that does not show this feature.

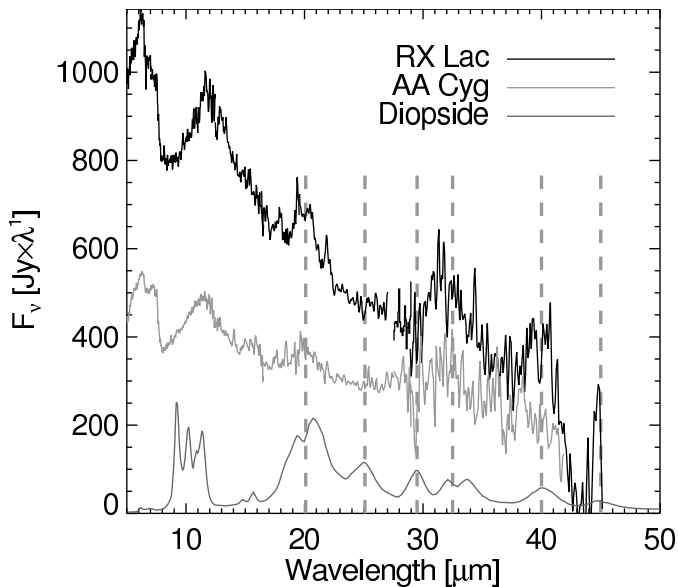


Figure 3. Long wavelength spectra of RX Lac and AA Cyg. The intensity units are chosen to better exhibit the emission bands on the steeply dropping stellar continuum. Below we show the absorption cross-sections of Diopside ($\text{MgCaSi}_2\text{O}_6$, Koike et al. 2000)

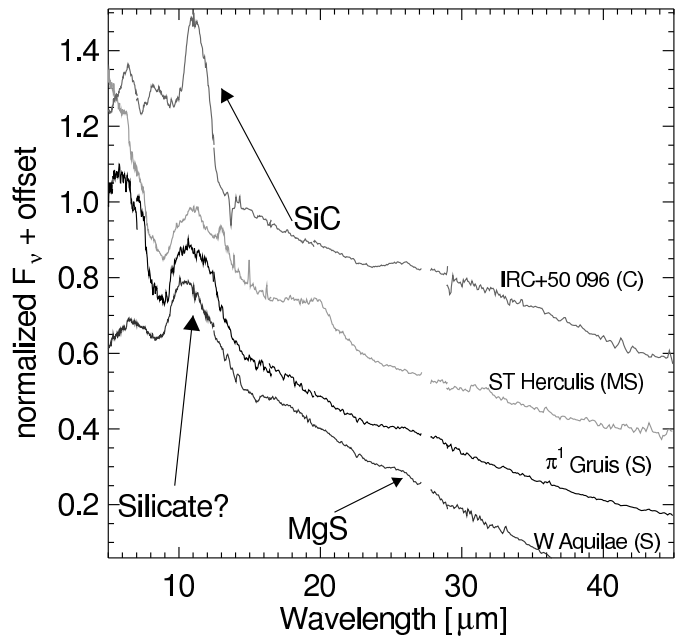


Figure 4. Overview of the SWS spectra of four red giant stars. We show from top to bottom the carbon-rich AGB star IRC+50 096, the M6.5S star ST Her and the S stars π^1 Gru and W Aql. The carbon-rich star exhibits the typical SiC feature at $11.3 \mu\text{m}$ and the MgS feature near $26 \mu\text{m}$. The ST Her spectrum is dominated by the silicate dust features at 10 and $20 \mu\text{m}$ which are typical for oxygen-rich environments. π^1 Gru and W Aql exhibit the MgS feature (see also Fig. 5 & 2) and a broad feature around $10 \mu\text{m}$ which resembles the silicate emission but is lacking clear evidence of the corresponding $20 \mu\text{m}$ silicate band. The latter is especially clear in the spectrum of π^1 Gru, while there is a weak feature near $\sim 17 \mu\text{m}$ in the spectrum of W Aql.

Comparing the detected features with available laboratory spectra they seem to correspond best to Diopside. There might be a connection between the appearance near $10 \mu\text{m}$ as both sources exhibit a weak, very red emission feature and strong SiO absorption. This absorption, in combination with a low Diopside temperature, might explain why we do not detect the corresponding $10 \mu\text{m}$ bands of Diopside. In should be borne in mind that the long wavelength spectra of these stars are quite noisy and that the correspondence with the laboratory spectrum is not perfect. In particular the $25 \mu\text{m}$ feature which is present in the laboratory spectrum is markedly absent in the stellar emissions. Therefore this should be considered a tentative identification.

4. The broad feature in the SWS spectra of S stars

The most prominent dust feature in the spectra of these S stars is the broad and smooth emission feature centred around $\sim 11 \mu\text{m}$ (Fig. 4 and the middle panel of Fig. 5). A similar feature (covering the same wavelength range) is found in the IR spectra of many O-rich evolved stars (e.g. Gillett et al. 1968; Little-Marenin & Little 1990; Kraemer et al. 2002), which it is usually attributed to a combination of silicates and aluminium-oxide with the possible addition of spinel at $13 \mu\text{m}$ (e.g. Woolf & Ney 1969; Hackwell 1972; Posch et al. 1999; Cami 2002). However, the corresponding silicate feature due to the Si-O stretch/bend near $18 \mu\text{m}$ is remarkably weak.

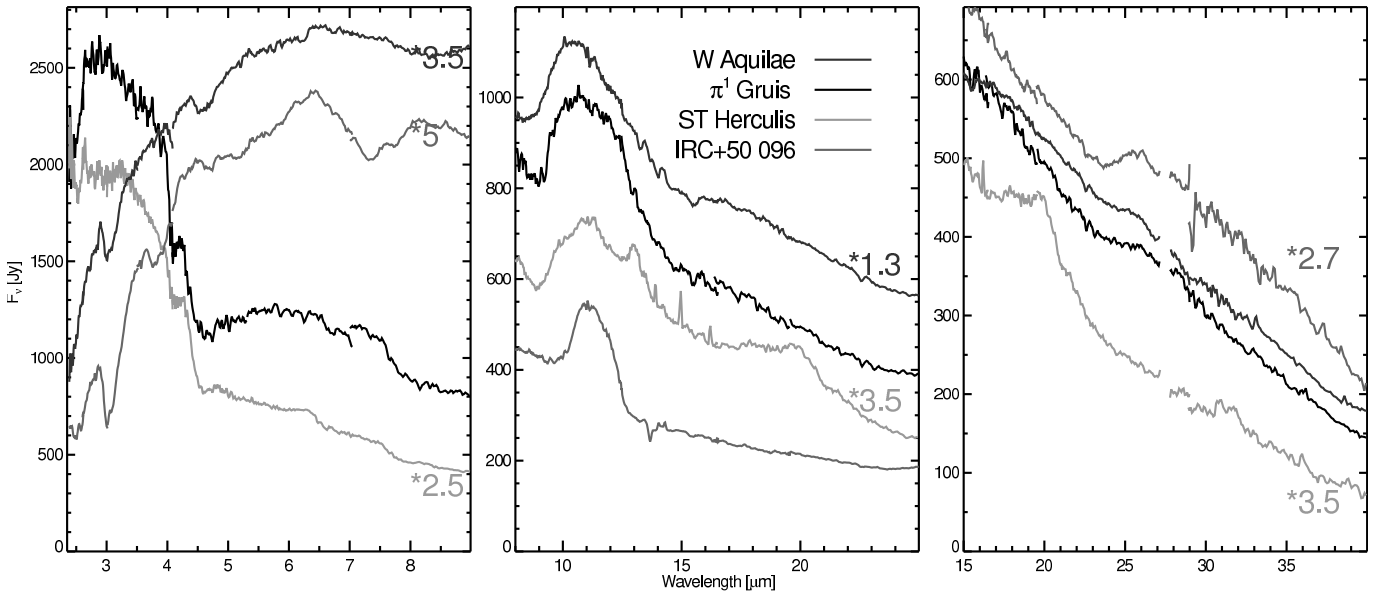


Figure 5. Detailed view of the IR spectra of the stars presented in Fig. 4. The left panel shows the shortest wavelength region in which the spectral structure is dominated by molecular absorption bands. Clearly the molecular composition of π^1 Gru resembles that of ST Her. The typical C-rich molecular bands due to C_2H_2 , HCN and C_3 are absent in π^1 Gru but are seen in the IRC+50 096 and W Aql. The middle panel compares the 10 to 20 μm range of these sources. The wavelength range of the broad $\sim 10 \mu\text{m}$ emission band in the S star spectra is identical to the silicate emission of ST Her, however the feature appears more smooth and the sharp substructures at 9.5, 10.8 and 13 μm are absent. Likewise, the 20 μm silicate band is not observed. The silicon-carbide feature seen in IRC+50 096 corresponds in peak position but is much narrower than the emission feature in ST Her. Finally, the panel on the right shows the MgS emission feature which is detected in the IR spectra of π^1 Gru, W Aql and IRC+50 096 and not in ST Her.

The similarities between the S star 10 μm features and the broad feature found in the O-rich spectra have until now been interpreted as the S stars showing silicate plus aluminium-oxide emission like the O-rich stars. In the following we will argue against this interpretation. Instead, we will show that there is a significant difference between the M star broad features due to silicates plus aluminium-oxide and the S star broad features, pointing to a different dust composition for these S stars. In the following we concentrate on comparing the S star spectra with O-rich stars that exhibit low dust columns, since these O-rich stars show the structured 10 μm emission complex. The stars that have higher mass-loss rates show profiles close to the classical silicate emission (e.g. Heras & Hony 2005). See TY Dra in Fig. 1 for an example of such a classical silicate feature.

We readdress the issue of the spectral appearance of the 8–22 μm dust spectra of the S stars using the available SWS spectra. We choose to restrict ourselves to the relatively small sample of SWS spectra for several reasons. The first reason is to have a consistent data set. More importantly, the sensitivity and spectral resolving power allow us to discuss details not available in the LRS spectra or in many of the ground-based spectra. As an example we mention R Aql for which Speck et al. (2000) report a broad feature without detectable substructure based on their CGS3 spectra, while the SWS spectra clearly resolve the substructures at 9.7, 11 and 13 μm . Finally, the much wider wavelength coverage allows us to better separate the different molecular and dust contributions. For example, the 10 μm region feature of the Mira variable RR Per resembles the S star spectra. However, the complete SWS spectrum reveals very strong molecular absorption and emission bands. This spectrum could have been misinterpreted, in case only the 8 – 22 μm range would have been available.

Kraemer et al. (2002) have classified the ISO/SWS spectra according to the shape of the continuum and dust features. Within their classification π^1 Gru, W Aql and many O-rich stars belong to the same class exhibiting the broad feature due to silicate and aluminium-oxide. Although the peak position and wavelength extend of the emission bump are indeed very similar, the O-rich sources show more substructure with often a prominent sharp emission maximum at 13 μm and always substructure at 9.7 and $\sim 11 \mu\text{m}$ (e.g. Cami 2002, see also Fig. 5). This substructure is not found in the spectra of π^1 Gru and W Aql.

A careful survey of all evolved star spectra with sufficient signal to noise in the SWS database yields 9 more sources with a broadened and smooth $\sim 10 \mu\text{m}$ emission feature. These sources are listed in Table 1 and their spectra are shown in Fig. 1. The main conclusion we draw is that such a broad and smooth emission feature is only found in the M super-giant and the S star spectra, *there are no O-rich AGB stars that exhibit the same emission feature*. This agrees very well with the findings of Speck et al. (2000) that the broad feature in the AGB stars differs from the broad features found in the super-giants. The ISO spectra show that in fact the broad O-rich AGB star features are always due to a mixture of the 9.7, 11 and 13 μm bands in which the 11 μm band dominates. Admittedly the substructures are sometimes more pronounced than in other cases which leaves open the possibility that part of the emission in this region, even in the O-rich AGB stars spectra, is due to the same smooth feature present in the S stars. χ Cyg is the only S star that has exhibits these substructures although the predominant contribution might still be a smooth underlying feature.

Note that the sample of M super-giants displayed in Fig. 1 largely overlaps with the broad featured M super-giants presented by Speck et al. (2000) and consists mostly of super-giants located in the h and χ Per association. These sources are by no

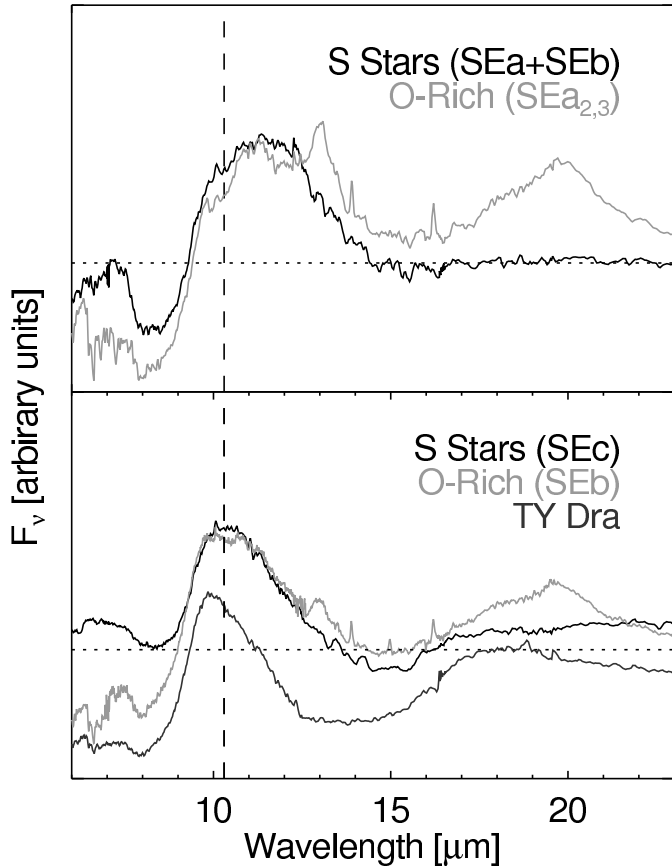


Figure 6. Comparison of the mean profiles of the S stars and the O-rich stars. The samples have been split in two parts. Those with profiles peaking beyond $10.5 \mu\text{m}$ (top panel) and those that peak at shorter wavelengths (bottom panel). The dashed line indicates the position ($10.3 \mu\text{m}$) where the mean profiles differ significantly. For reference we also show the feature spectrum of TY Dra, which shows a classical silicate emission feature. The spectrum has been offset for clarity.

means typical for all galactic M super-giants. As we already pointed out, the large majority of studied M super-giants exhibits a classical silicate emission feature (Sloan & Price 1998; Speck et al. 2000). Moreover, seven out of the nine broad featured M super-giants in our sample reveal UIR emission bands, which are not commonly found in the M super-giant spectra (Sylvester et al. 1994, 1998). Sylvester et al. (1998) suggest that this could be related to peculiar elemental abundances at the stellar surfaces.

Another striking aspect of these spectra as a group is the relative strength of the $10 \mu\text{m}$ feature compared to the $18 \mu\text{m}$ feature. In the spectra of the O-rich stars, the $10 \mu\text{m}$ emission is accompanied by an emission feature near $18\text{--}20 \mu\text{m}$, where one would expect the Si-O bending modes of the silicates to be present (see Fig. 5). This emission band is systematically weak in the M super-giant and S star spectra in Fig. 1. In some of the sources we find no evidence of the $18 \mu\text{m}$ band at all and three sources exhibit a weak emission band near $15 \mu\text{m}$ instead.

4.1. Feature extraction

The differences in the observed features as discussed above are relatively subtle. In order to enhance the contrast we have removed the “continuum” from the spectra. We stress that the

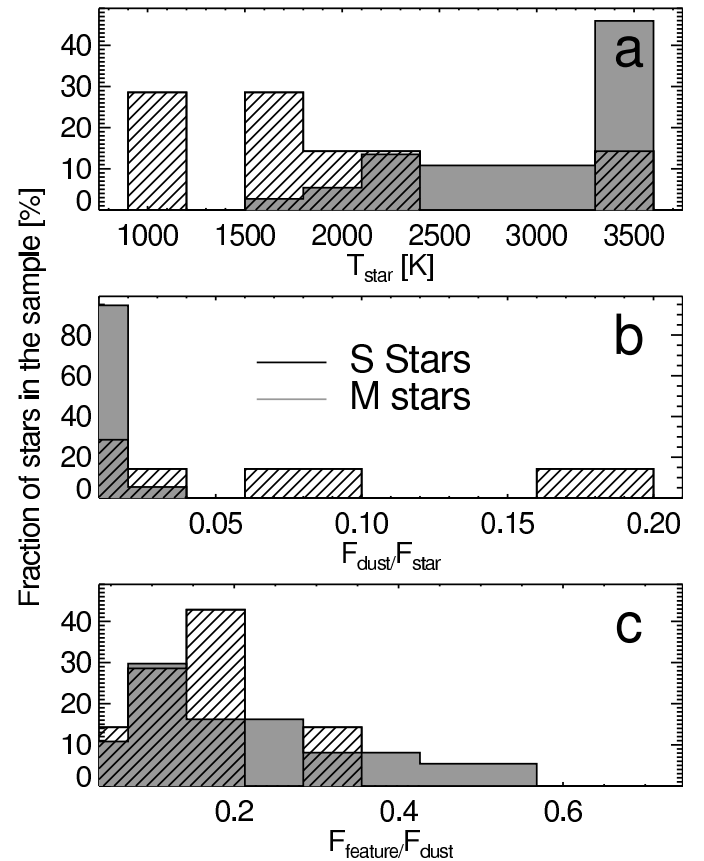


Figure 7. Properties of the M and S stars. From top to bottom: the fitted temperature of the (reddened) stars; the ratio of the excess to the stellar flux and the ratio of the flux in the feature to the flux in the dust excess. The S stars in the sample are clearly cooler (i.e. more extinguished) and show more excess than the M stars.

continuum as such does not have any clear physical meaning in this context as the same material(s) that give rise to the features contribute to this continuum. It represents only a means to remove those contributions that do not give rise to spectral signatures. It further allows us to compare the relative strength of the remaining bands to other components. Because of the wide range of properties of the stars in the sample – in terms of optical depth, strength of the molecular bands and the excess – we have opted to use a crude method for continuum estimation. The continuum is represented by a sum of a warm black-body-function ($F_\nu = B_\nu(T)$; the reddened stellar photosphere) and a cooler modified black-body-function ($F_\nu = \nu^p \times B_\nu(T)$; the dust excess). These two functions are fitted simultaneously to selected “continuum-points”. The latter are difficult to define unambiguously and we choose to use the following ranges: $2.9\text{--}3.35 \mu\text{m}$, when the molecular absorption is not too prominent; $3.35\text{--}3.8 \mu\text{m}$; $7\text{--}7.5^\dagger \mu\text{m}$; $8.5\text{--}9.5^\dagger \mu\text{m}$; $14\text{--}15 \mu\text{m}$; $22\text{--}25 \mu\text{m}$ and $36\text{--}44 \mu\text{m}$. The ranges marked with a dagger often do not exhibit clear continuum character. These regions have still been included, albeit with a reduced weight, to account for the fact that the continuum should run close to them.

The resulting residual spectra have been co-added to reduce the noise. The co-addition has been applied in two bins, depending on the peak-position of the “ $10 \mu\text{m}$ ” emission feature. The results are shown in Fig. 6, where we compare the S star profiles to the features found in O-rich stars. Note that the comparison

is done on the basis of the extracted feature and does not follow strictly the silicate-index classification. We find that both S-star SEa and SEb classes compare best with the O-rich SEa class and the S-star SEc class with the O-rich SEb class. This mismatch reflects the fact that the underlying continua differs systematically – the O-rich stars being bluer – between both groups of sources (see also below).

Fig. 6 demonstrates that indeed the O-rich star exhibit a “10” μm feature which is composed of three distinct components while the S star spectra exhibit only a single broad emission band – indicative of a different dust composition between the two groups. There are several other “properties” of these dust spectra that change in league with the differences in dust composition. The lack of the 19.5 μm band in the S star spectra is pronounced. In Fig. 7 we summarise the derived properties of the S stars compared to those of the M stars. The main conclusion is that the studied S stars as a sample are redder and exhibit a stronger excess than the O-rich stars with the broad 10 μm feature. This indicates the presence of more dust along the line of sight towards the S stars. There is no significant difference in the strength of the 10 μm feature relative to the dust continuum (Fig. 7c).

5. Discussion

As discussed above, the spectral appearance of S stars is significantly different from the O-rich AGB stars. Here we explore the possible explanations for these differences, that is, the relative strength of the emission bands and the displacement of the 10 μm feature. The amount of mid-IR excess is probably not directly related to the dust composition. Perhaps the observed difference in dust composition and the differences in the quantities of dust share a common origin in the particular condition that prevail during the S star evolutionary state.

There are several effects that, if at work, will influence the spectral appearance of dust features even arising from grains with the same chemical composition. The most notable are dust temperature and grain-size. Using the amorphous olivine ($\text{Mg}_{0.8}\text{Fe}_{1.2}\text{SiO}_4$) that explains (part of) the emission of the O-rich stars well (Heras & Hony 2005)), we find that the temperature required to explain the observed S star 10-to-18 μm ratio (ignoring the mismatch in peak-position) needs to be higher than 2000 K. And even at such high temperatures (well above the evaporation temperature of silicates) the feature at 18 μm would still be too prominent for the most extreme cases, e.g. π^1 Gru or W Aql. Thus, dust temperature is excluded as the cause of the weak 18-20 μm features.

Grain-size: We have simulated the effects of grain-size on the spectral features of silicates based on simulated optical properties using a Mie calculation (Bohren & Huffman 1983). The effect of increasing the grain-size from 0.01 to 1 μm is indeed a displacement of the 10 μm emission feature, but the effect is subtle and it moves the peak by less than 0.3 μm . This is not enough to explain the S star spectra. Moreover the ratio of the 10 to 18 μm band is only slightly affected. The 18 μm band does not shift significantly but becomes somewhat stronger. The S star spectra exhibit an 18 μm feature which is little pronounced and peaks at shorter wavelength. We conclude that the grain-size is not the dominant factor for explaining the S star silicate feature.

The paper by Jäger et al. (2003) is very interesting in terms of the compositional influence on the silicate emission. These authors have studied the IR transmission spectra of non-stoichiometric magnesium-rich silicates. They find that there is a significant shift of the 10 μm Si-O stretching resonance as a

function of the Mg to SiO_4 ratio. The trend is such that as the Mg to SiO_4 ratio increases, the 10 μm peak shifts to longer wavelength, the 18 μm band broadens and weakens compared to the continuum and shifts to shorter wavelength. This mimics to a large extent the behaviour observed in the S star spectra. It should be noted that although the 10 μm feature in the laboratory spectra shifts by a large amount ($>1 \mu\text{m}$), it is not completely sufficient to explain the full range observed in the stellar spectra. If the observed shift is indeed linked to the presence of non-stoichiometric silicates, than there could be an obvious connection to the photospheric abundances since the Mg to SiO_4 ratio in the silicate might measure the Mg to free O or SiO in the gas phase. In case of $\text{C/O} \sim 1$ there is more Mg in relative terms and those non-stoichiometric silicates may form.

Moreover, the M-super-giants that we present are special not just in their 10 μm spectrum but also because they exhibit a dual chemistry with both silicates and PAHs. How this dual chemistry comes about is at present unclear. This may be evidence of the presence of a disk plus wind geometry, shocked regions in the outflow or an abundance pattern in the outflow, which permit this dual chemistry to exist. In any case, it is clear that in some region of the circumstellar environment the chemistry should be close to a C/O around unity.

It should be stressed that we cannot draw general conclusions about the dust formation around S stars from such a small number of sources. We have successfully proposed to observe 90 S stars with IRS Houck et al. (2004) on Spitzer (GO-30737, PI. Hony). The main findings of the current paper, i.e., the presence of the MgS feature and the shifted 10 μm feature, are borne out by the spectra obtained in the Spitzer sample (Smolders et al. in prep). Because of the larger sample the range of spectral features, in particular in the 10-20 μm region is larger than what is presented here.

6. Conclusions

We have presented a detailed study of dust spectra of the S stars observed by ISO/SWS. The spectra exhibit several unique dust characteristics. In particular, we find two S stars (π^1 Gru and W Aql) that exhibit a weak “30” μm feature due to MgS grains. RX Lac and AA Cyg exhibit features between 20–40 μm which may be related to Diopside, although this is at most a tentative identification. The 10 μm region of the dust-producing S stars stands out due to its smooth and broad emission feature. The feature is located clearly at longer wavelengths than the classical silicate feature, without showing the characteristic substructure found in the spectra of the O-rich AGB stars with a broad 10 μm feature. The peculiar 10 μm features of the S stars are accompanied by very weak or absent features near 18 μm . We conclude that S stars make different types of dust than the O-rich AGB stars, including those that exhibit shifted 10 μm features. As a group the S stars and their dust shells do not compare well to the O-rich AGB stars with structured features, the S stars are redder and produce more dust. The common explanation for the shifted 10 μm band, i.e. a mixture of classical silicate with aluminium-oxide, does not appear to apply to the S stars. We have explored possible origins of the peculiar spectra. We find that non-stoichiometric silicates with an increased Mg to SiO_4 ratio might be at the origin of the displaced emission. Interestingly, the properties of the peculiar 10 and 20 μm features are shared with a small subgroup of M super-giants. These super-giants, which are preferentially found in the h and χ Per associations, also exhibit the UIR emission features, again

strengthening the possible link with the abundances in the dust forming regions.

Acknowledgements. IA³ is a joint development of the SWS consortium. Contributing institutes are SRON, MPE, KUL and the ESA Astrophysics Division. This work was supported by the Dutch ISO Data Analysis Center (DIDAC). The DIDAC is sponsored by SRON, ECAB, ASTRON and the universities of Amsterdam, Groningen, Leiden and Leuven.

References

- Blanco, V. M. 1955, *ApJ*, 122, 434
 Bohren, C. F. & Huffman, D. R. 1983, *Absorption and scattering of light by small particles* (New York: Wiley, 1983)
 Buscombe, W. 1998, *VizieR Online Data Catalog*, 3206, 0
 Buscombe, W. 2001, *VizieR Online Data Catalog*, 3222, 0
 Cami, J. 2002, PhD thesis, University of Amsterdam
 Chen, P. S. & Kwok, S. 1993, *ApJ*, 416, 769
 Clegg, P. E., Ade, P. A. R., Armand, C., et al. 1996, *A&A*, 315, L38
 de Graauw, T., Haser, L. N., Beintema, D. A., et al. 1996, *A&A*, 315, L49
 Egan, M. P. & Sloan, G. C. 2001, *ApJ*, 558, 165
 Ferrarotti, A. S. & Gail, H.-P. 2002, *A&A*, 382, 256
 Gillett, F. C., Low, F. J., & Stein, W. A. 1968, *ApJ*, 154, 677
 Hackwell, J. A. 1972, *A&A*, 21, 239
 Heras, A. M. & Hony, S. 2005, *A&A*, 439, 171
 Houck, J. R., Roellig, T. L., Van Cleve, J., et al. 2004, *American Astronomical Society Meeting Abstracts*, 204
 Humphreys, R. M. 1970, *AJ*, 75, 602
 Jäger, C., Dorschner, J., Mutschke, H., Posch, T., & Henning, T. 2003, *A&A*, 408, 193
 Kessler, M. F., Steinz, J. A., Anderegg, M. E., et al. 1996, *A&A*, 315, L27
 Kharchenko, N. V. 2001, *Kinematika i Fizika Nebesnykh Tel*, 17, 409
 Koike, C., Tsuchiyama, A., Shibai, H., et al. 2000, *A&A*, 363, 1115
 Kraemer, K. E., Sloan, G. C., Price, S. D., & Walker, H. J. 2002, *ApJS*, 140, 389
 Little-Marenin, I. R. & Little, S. J. 1988, *ApJ*, 333, 305
 Little-Marenin, I. R. & Little, S. J. 1990, *AJ*, 99, 1173
 Lorenz-Martins, S. & Pompeia, L. 2000, *MNRAS*, 315, 856
 Miyata, T., Katata, H., Okamoto, Y., Onaka, T., & Yamashita, T. 2000, *ApJ*, 531, 917
 Onaka, T., de Jong, T., & Willems, F. J. 1989, *A&A*, 218, 169
 Posch, T., Kerschbaum, F., Mutschke, H., et al. 1999, *A&A*, 352, 609
 Skinner, C. J., Griffin, I., & Whitmore, B. 1990, *MNRAS*, 243, 78
 Sloan, G. C., Kraemer, K. E., Price, S. D., & Shipman, R. F. 2003, *ApJS*, 147, 379
 Sloan, G. C. & Price, S. D. 1995, *ApJ*, 451, 758
 Sloan, G. C. & Price, S. D. 1998, *ApJS*, 119, 141
 Solf, J. 1978, *A&AS*, 34, 409
 Speck, A. K., Barlow, M. J., Sylvester, R. J., & Hofmeister, A. M. 2000, *A&AS*, 146, 437
 Stephenson, C. B. 1994, *VizieR Online Data Catalog*, 3168, 0
 Stephenson, C. B. 1995, *VizieR Online Data Catalog*, 3060, 0
 Sylvester, R. J. 1999, *MNRAS*, 309, 180
 Sylvester, R. J., Barlow, M. J., & Skinner, C. J. 1994, *MNRAS*, 266, 640
 Sylvester, R. J., Skinner, C. J., & Barlow, M. J. 1998, *MNRAS*, 301, 1083
 Winfrey, S., Barnbaum, C., Morris, M., & Omont, A. 1994, *Bulletin of the American Astronomical Society*, 26, 1382
 Woolf, N. J. & Ney, E. P. 1969, *ApJ*, 155, L181
 Yang, X. H., Chen, P., Wang, J., & He, J. 2007, *A&A*, 463, 663

List of Objects

- ‘ π^1 Gru’ on page 4
- ‘W Aql’ on page 4
- ‘RX Lac’ on page 4
- ‘IRC+50 096’ on page 4
- ‘ST Her’ on page 4
- ‘R Aql’ on page 6
- ‘RR Per’ on page 6
- ‘ π^1 Gru’ on page 8
- ‘W Aql’ on page 8
- ‘AA Cyg’ on page 8